Formation of Single-Wall Carbon Nanotubes: Comparison of CO_2 Laser Ablation and Nd:YAG Laser Ablation

M. Yudasaka,*,† F. Kokai,‡ K. Takahashi,‡ R. Yamada,† N. Sensui,† T. Ichihashi,§ and S. Iijima†,§

ICORP-JST, Nanotubulites Project, c/o NEC Corporation, 34 Miyukigaoka, Tsukuba 305-8501, Japan, Institute of Research and Innovation, 1201 Takada, Kashiwa, Chiba 277-0861 Japan, and NEC Fundamental Research Laboratory, 34 Miyukigaoka, Tsukuba 305-8501, Japan

Received: January 6, 1999; In Final Form: March 8, 1999

Investigating the formation of single-wall carbon nanotubes (SWNTs) from a target composed of graphite, Ni, and Co, we compared the use of a pulsed CO_2 laser (pulse width of 20 ms, laser-power density of 0.1 MW/cm^2) with the use of a pulsed Nd:YAG laser (pulse width of 5−7 ns, laser-power density of 4 GW/cm^2). When the total irradiation energy was 2 kW/cm^2 for the CO_2 laser ablation and 2.4 kW/cm^2 for the Nd:YAG laser ablation, SWNTs could be formed at 300 K by CO_2 laser ablation, whereas the lowest temperature at which they could be formed by Nd:YAG laser ablation was about 1170 K. The lowest pressure allowing SWNT formation was 50 Torr for CO_2 laser ablation and 200 Torr for Nd:YAG laser ablation. The structures of carbonaceous deposits and of the target surfaces indicated that CO_2 laser ablation resulted in carbon being emitted from the edges of or defects in the graphite particles and most of the Ni and Co being emitted from the target. Pulsed Nd:YAG laser ablation, on the other hand, has been reported to result in graphite melting and mixing with Ni and Co on the target surface, the mixture being expelled from the target surface, and clumps of Ni and Co remaining on the target surface after the laser ablation. We think these differences are due to the different laser-power densities and pulse widths.

Introduction

Research on single-wall carbon nanotubes (SWNTs) has continued since they were first found by Iijima in 1993.[1] Purification methods have been proposed and used to obtain high-purity SWNTs[2] that have been used in fundamental research. However, a critical problem in fundamental research, as well as in the development of applications, is that there has not been an appropriate method for high-yield mass production of SWNTs. Two well-known methods used to produce relatively large amounts of SWNTs are the arc-discharge method[3] and the laser-ablation method.[4] To develop a mass production method, though, we need to understand the mechanisms by which these methods form SWNTs. The arc in the arc discharge cannot be controlled, and laser ablation using a Nd:YAG pulsed laser must be performed at high temperatures, usually above 1200 K. These conditions have made SWNT formation hard to observe in situ, so the formation mechanisms have been deduced from the structure of the SWNTs[5−8] and, in our study, also from the structures of target surfaces and the non-SWNT carbonaceous products.[9,10]

Laser ablation using a CO_2 laser under continuous-wave operation has recently made it possible to form SWNTs at room temperature.[11] Since high temperatures of above 1200 K are necessary to make SWNTs by Nd:YAG laser ablation, we think that comparing the SWNT formation method using a CO_2 laser with the method using a Nd:YAG laser will help us understand more about the SWNT formation mechanism.

† ICORP-JST.
‡ Institute of Research and Innovation.
§ NEC Fundamental Research Laboratory.

TABLE 1: Irradiation Conditions of CO_2 and Nd:YAG Laser Beams Used for SWNT Formation

	pulse width	wave-length	laser power density	total irradiation energy, W/cm^2	no. of pulses	beam diameter, mm
CO_2 laser	20 ms	10. 6 μm	0.1 MW/cm^2	2000	1	1
Nd:YAG laser	5−7 ns	532 nm	4 GW/cm^2	2400	600	4

TABLE 2: Comparison of SWNT Formation Conditions (Temperature, T_{SWNT}; Pressure, P_{SWNT}) and Characteristics of Target Surfaces When CO_2 and Nd:YAG Lasers Were Used[a]

	T_{SWNT} (K)	P_{SWNT} (Torr)	materials at target surface after laser-beam irradiation
CO_2 laser	>300	>50	Ni, Co: none remaining C: graphite
Nd:YAG laser	>1170	>200	Ni, Co: some remaining C: a-C

Experimental Section

The chamber used for the laser ablation is described in detail in our previous report.[9] It had a cylindrical shape, an inside diameter of about 3.6 cm, and a length of 60 cm. The window for the CO_2 laser beam inlet was a ZnSe plate and the window for the Nd:YAG laser beam inlet was a quartz-glass plate. A quartz-glass tube with an inside diameter of about 2.7 cm and a length of 50 cm was located at the center of the chamber, and a target was placed at the center of the quartz-glass tube. The target was a compressed powder that was a mixture of graphite, Ni, and Co particles with sizes of 5−10 μm. The atomic

10.1021/jp990072g CCC: $18.00
Published on Web 04/20/1999

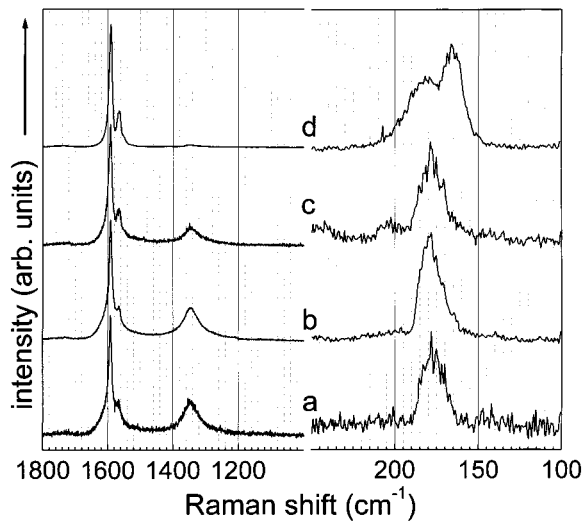

Figure 1. Raman spectra of carbonaceous deposits formed by CO_2 laser ablation at temperatures of (a) 300 K, (b) 670 K, (c) 1070 K, and (d) 1470 K.

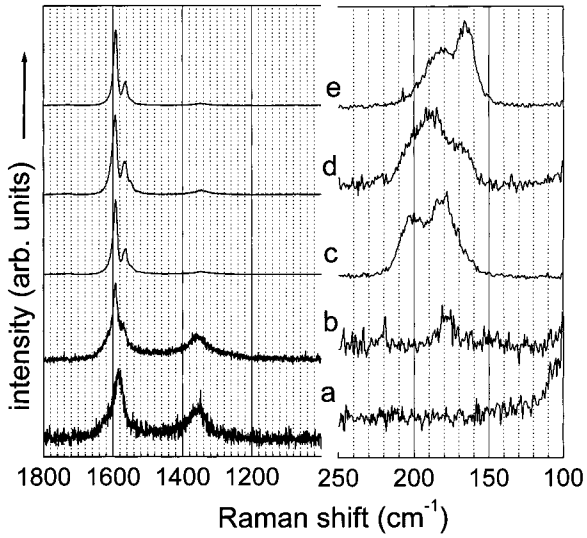

Figure 2. Raman spectra of carbonaceous deposits formed by CO_2 laser ablation at pressures of (a) 4 Torr, (b) 50 Torr, (c) 100 Torr, (d) 400 Torr, and (e) 600 Torr.

percentage of C, Ni, and Co was 98.8:0.6:0.6. Before the laser ablation, the targets were heat treated at 1470 K for 30 min. After the heat treatment, Ni and Co metal particles were alloyed, and the alloyed Ni−Co particles had a Ni/Co ratio of 30−70% and sizes of about 10−30 μm. A quartz-glass plate was situated in front of the target. The temperature at and around the target was raised by using an electric furnace that surrounded the chamber. Argon gas flowed through the tube at 0.5 L/min, and the pressure inside the chamber was kept at a level between 4 and 600 Torr.

A CO_2 laser beam or Nd:YAG laser beam irradiated the target surface perpendicularly. (Beam conditions are listed in Table 1.) The direction of the laser-beam irradiation was the same as that of the Ar gas flow.

Results

Raman spectra of the carbonaceous deposits formed at various temperatures are shown in Figure 1. The peaks at 1592, 1565, and 160−180 cm^{-1} in Figure 1 are characteristic of SWNTs.[12] The positions of the peaks in the range 160−180 cm^{-1} (breathing-mode vibration) indicate that the diameter of SWNTs is 1.3−1.4 nm.[12] The broad peaks at 1350 and 1590 cm^{-1} are

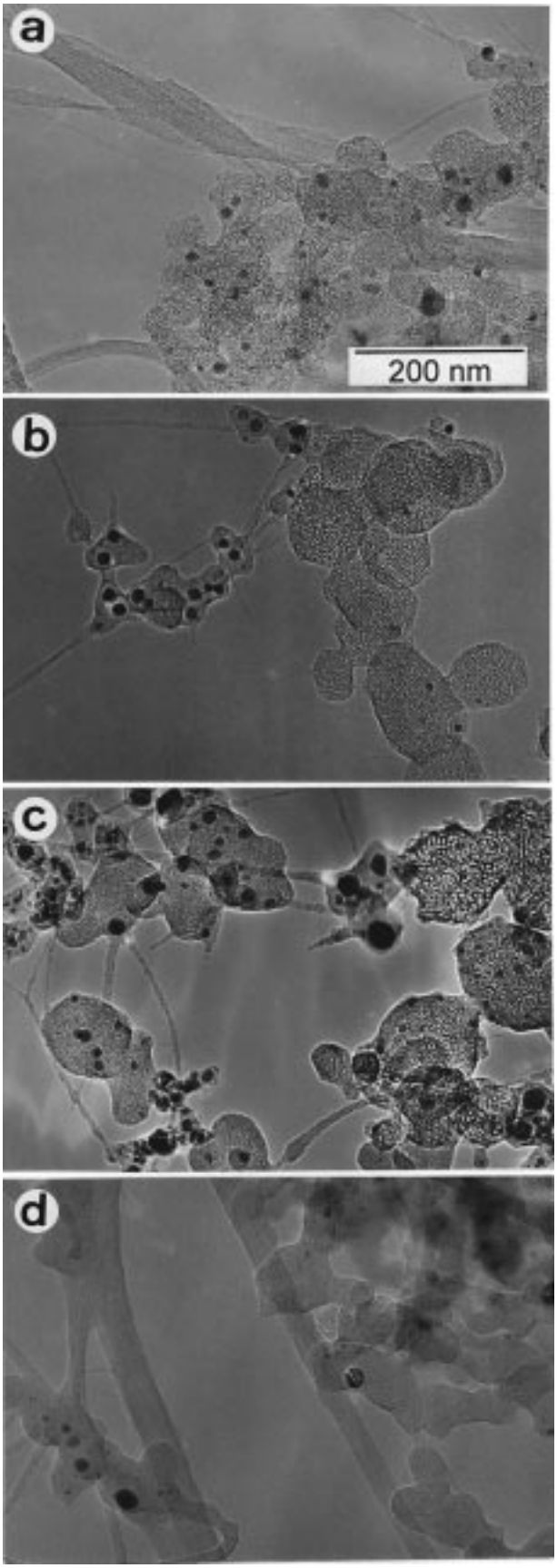

Figure 3. Transmission electron microscope images of the carbonaceous deposits formed at (a) 1470 K under 600 Torr, (b) 670 K under 600 Torr, (c) 300 K under 600 Torr, and (d) 1470 K under 100 Torr.

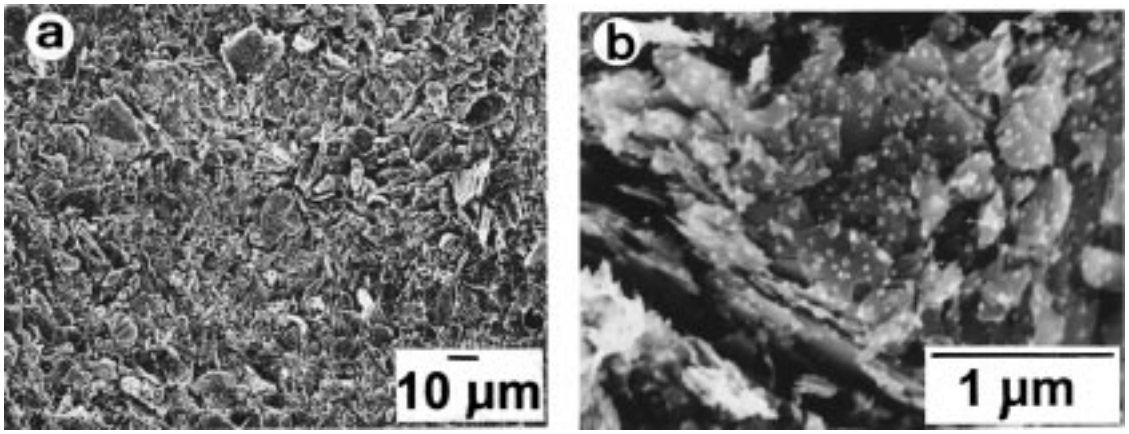

Figure 4. Scanning electron microscope images of target surfaces after CO_2 laser ablation at 1470 K under 600 Torr.

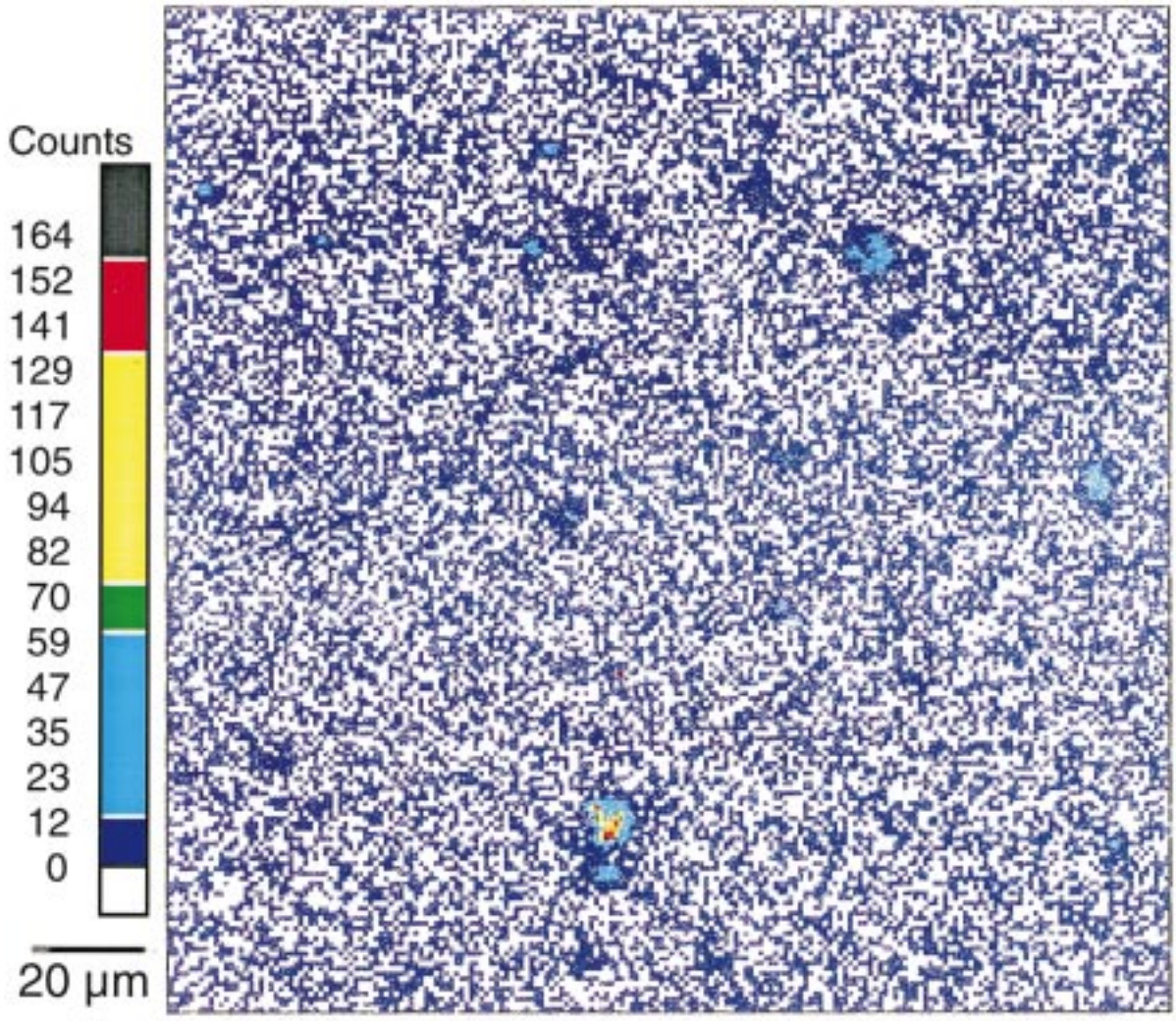

Figure 5. EPMA analysis for Ni distribution at the target surface after CO_2 laser ablation. (Co was found at almost the same places as Ni.)

mainly due to single-wall carbon nanohorn (SWNH) aggregates.[13] The temperature dependence of the spectra in Figure 1 shows that SWNTs can be formed at room temperature (about 300 K) (Table 2) and that the quantity of SWNTs relative to that of SWNHs increases with increasing temperature. Although the position, intensity, and number of peaks appearing in the range of 160−180 cm^{-1} and the intensities of the broad peaks at 1350 and 1590 cm^{-1} depended on the measuring spot in each specimen, there was a definitive tendency for the peaks of SWNTs to become larger as the temperature increased.

The Raman spectra of the carbonaceous deposits formed at 1470 K under various Ar gas pressures also depended on the measuring spots of the specimen when the pressure was at and above 50 Torr (Figure 2). However, several inherent tendencies can be seen in Figure 2. The spectra in Figure 2 indicate that SWNTs are formed when the pressure is above 50 Torr. The quantity of SWNTs relative to that of SWNHs does not much depend on the pressure when the pressure is above 200 Torr. The carbonaceous deposit formed at 4 Torr is graphitic since it shows a peak at 1580 cm^{-1} (Figure 2a) that is characteristic of

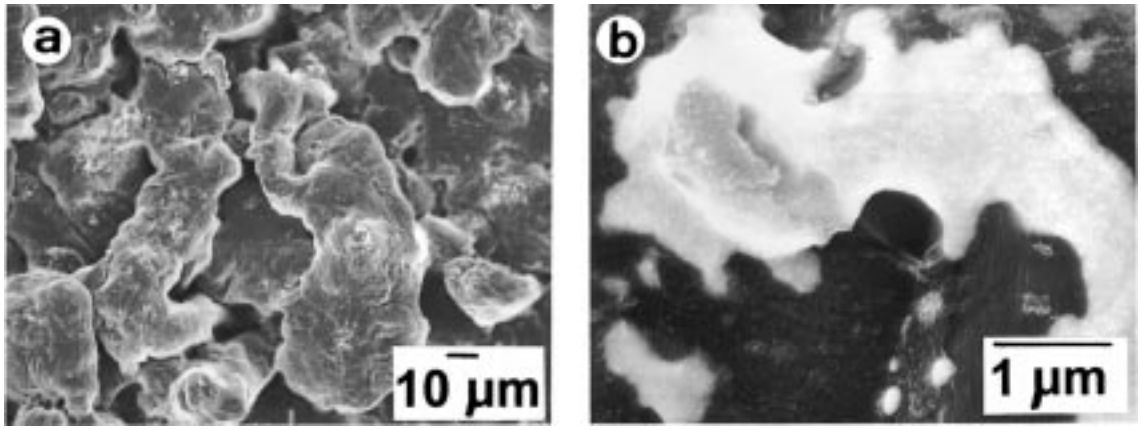

Figure 6. Scanning electron microscope images of target surfaces after Nd:YAG laser ablation at 1470 K under 600 Torr.

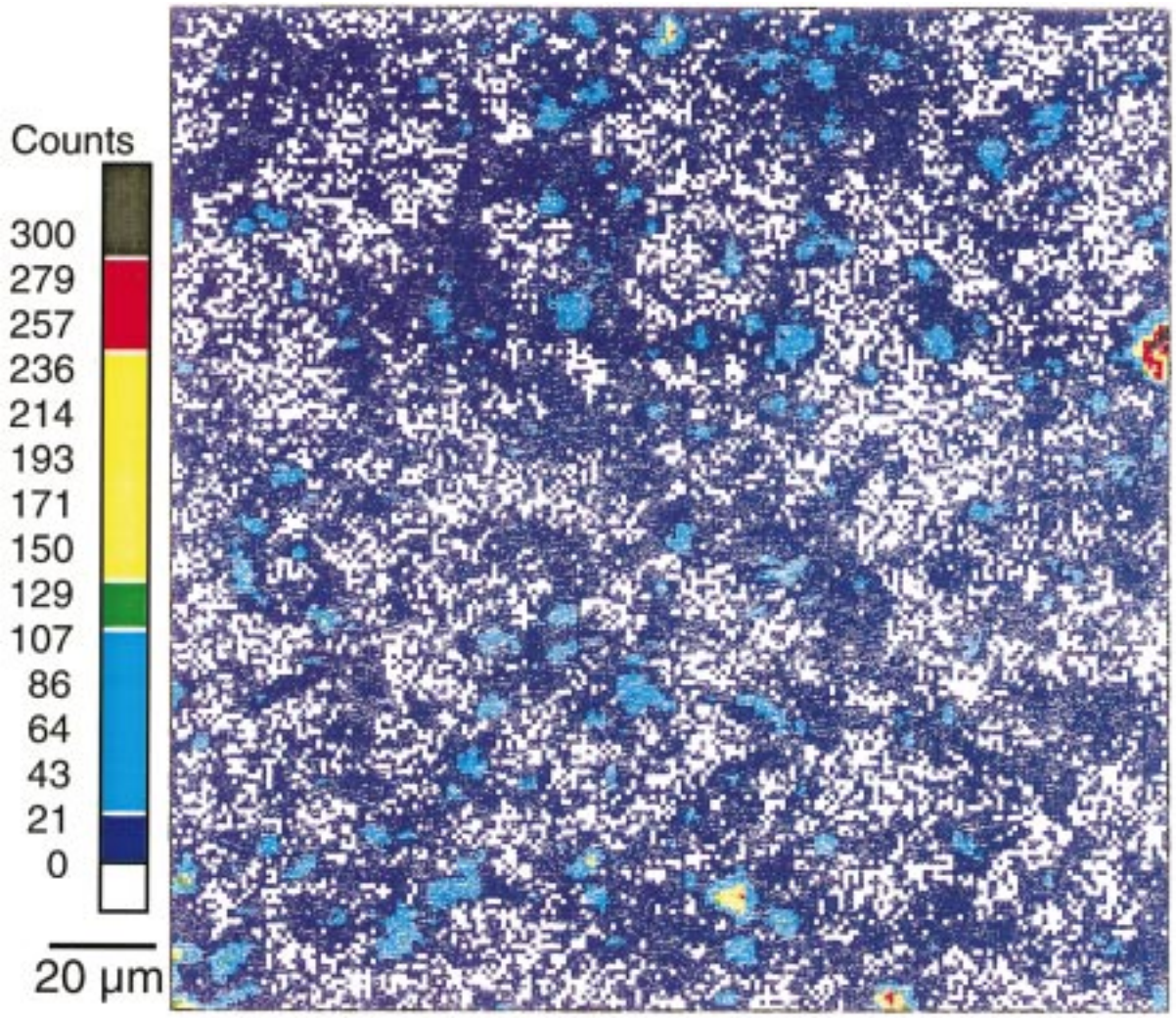

Figure 7. EPMA analysis for Ni distribution at the target surface after Nd:YAG laser ablation. (Co was found at almost the same places as Ni.)

graphite.[14] We confirmed by EPMA (electron probe microanalysis) measurements that this graphite formed at 4 Torr contained Ni and Co, which we think catalyzed the graphite formation.

Transmission electron microscope (TEM) images of the carbonaceous deposits formed at 1470 K under 600 Torr (e.g., Figure 3a) show SWNTs forming thick bundles. At an intermediate temperature, for example, 670 K, the TEM image shows SWNT bundles, amorphous carbon (a-C) particles from which SWNTs appears to grow, the SWNH aggregates, and metal (Ni, Co) particles embedded within particles of a-C and SWNH aggregates (Figure 3b). The SWNTs do not grow from SWNH aggregates. The TEM image of the carbonaceous deposits formed at room temperature under this pressure (Figure 3c) shows more round aggregates of SWNHs than it does SWNTs. A considerable quantity of SWNTs can be seen, though, in the TEM image of the carbonaceous deposits formed at 1470 K under 100 Torr (Figure 3d). We also observed particles of a-C and metal, but not SWNH aggregates. (The absence of SWNH aggregates in the carbonaceous products formed under low

pressure, for example, 4 Torr, coincides with the results we recently reported.[13])

According to our earlier study of SWNT formation by Nd:YAG pulsed laser ablation,[10] the temperature and pressure ranges in which SWNT formation was confirmed by Raman spectra were above 1170 K at under 600 Torr and above 200 Torr at 1470 K (Table 2). The TEM image of the carbonaceous deposit formed at 1470 K under 200 Torr showed a small quantity of short SWNTs.[9] Peaks appeared in the Raman spectra at 1592 and 1565 cm^{-1} and in a range from 165 to 200 cm^{-1}.[9,10] The peak position of the breathing mode did not depend on the measuring spot in each specimen, indicating that the distribution of the SWNT diameters was uniform.

The difference between the results obtained using a CO_2 laser and those obtained using a Nd:YAG laser (Table 2) can be ascribed to the different ways in which carbon and metals are emitted from the target. A scanning electron microscope (SEM) image of the target surface after CO_2 laser irradiation at 1470 K under 600 Torr (Figure 4a) shows graphite particles of the same sizes as those before the laser-beam irradiation. A more magnified image (Figure 4b) shows that each graphite particle had a layered structure and their layer edges were etched. The small particles with sizes of about 0.1 μm seen in Figure 4b were made of carbon, as was confirmed by EPMA analysis. The Raman spectrum of the target surface after the laser ablation showed two sharp peaks inherent to graphite at 1582 and 1350 cm^{-1}.[14] Since these two peaks were the same as those of the graphite particles contained in the original target, it is apparent that the graphite particles did not change into, for example, a-C but kept their graphite structure during the laser ablation. These results indicate that the C was emitted from the edges of or defects in the layers of the graphite due to the CO_2 1aser irradiation. Our EPMA analysis of the target surface subjected to the laser ablation indicated that there were some Ni particles whose size and number were close to those of the initial target (Figure 5). (Since Co coexisted with Ni, we do not show the EPMA data for the Co distribution here.) This indicates that the Ni and Co metals did not accumulate on but were emitted from the target surface during the CO_2 laser ablation.

The morphology of the target-surface ablated by Nd:YAG laser irradiation was very different from that for the CO_2 laser ablation. SEM images of the target surface show that the graphite and metal there were melted (Figure 6a).[9,10] Raman spectra of the laser-ablated surfaces showed two broad peaks characteristic of a-C near 1600 and 1350 cm^{-1}.[14] The magnified SEM image (Figure 6b) shows white islands; EPMA measurement indicated that these white particles were made of Ni and Co. The EPMA observations of the target surface subjected to the Nd:YAG laser ablation showed that the quantity of particles containing Ni (Figure 7) was greater than that for the CO_2 laser ablation (Figure 5). These results indicated that the Nd:YAG laser irradiation melted graphite and metal at the target surface, changing them into a-C and into metal islands.[9,10]

Discussion

A probable reason why the temperature and pressure ranges suitable for SWNT formation by CO_2 laser ablation are wider than those for SWNT formation by Nd:YAG laser ablation is as follows. The energy of the Nd:YAG laser absorbed by graphite was converted mostly to heat. (The reflection coefficient of graphite for light with a wavelength of 532 nm is 0.2.[15]) Since the Nd:YAG laser had a pulse width of 5−7 ns and a laser-power density of the gigawatt-per-square-centimeter order (Table 1), the temperature of the target graphite within the laser-irradiated area (0.07 cm^2) would increase to over 3000−4000 K during the laser-irradiated period.[16,17] (The propagation depth of the heat during the 5−7ns of irradiation has been estimated to be about 1 μm.[18−20]) This sudden elevation of the local temperature would cause the melted C to be abruptly emitted. At the same time, recoil pressure would be exerted on the molten C at the target surface, causing the molten C to be expelled from the target in the form of molten droplets.[21,22] When the Ar pressure was low, the molten C would be expelled from the target surface at once, without transferring heat to the metals in the target. Only when the pressure was high (and the emission rate was therefore low) and the ambient temperature elevated (and the metal could therefore melt easily) could the molten C make a mixture with the metal prior to the molten mixture of C and metal being expelled from the target surface in the form of droplets.[9]

Since the laser-power density of the CO_2 laser was less than 1 MW/cm^2 the pulse width was longer at 20 ms, we think the light absorbed by the graphite was converted to heat that diffused into the target and slowly elevated the temperature of a large volume of the target. (The reflection coefficient of graphite for light with a wavelength of 10.6 nm is 0.6. The propagation depth of the heat during the 20 ms of irradiation has been estimated to be about 2 mm.[18−20]) The volume in which the temperature rose was larger, and the highest temperature reached at the target surface was therefore lower than those in the case of the Nd:YAG laser ablation. Under these conditions, the heat would transfer from graphite to metal regardless of the ambient temperature or ambient pressure, and as a result, the temperature of the metal would rise high enough to allow the metal to be emitted from the target surface over wide ranges of ambient temperature and pressure. This must be a major reason why the CO_2 laser made it possible to expel not only C but also metal, which enabled the formation of SWNTs at lower temperatures and lower pressures than with the Nd:YAG laser.

References and Notes

(1) Iijima, S.; Ichihasshi, T. *Nature* **1993**, *363*, 603.

(2) Tohji, K.; Goto, T.; Takahashi, H.; Shinode, S.; Shimizu, N.; Jeyadevan, B.; Matsuoka, I.; Saito, Y.; Ohsuna, T.; Hiraga, K.; Nishina, Y. *Nature* **1996**, *383*, 679.

(3) Journet, C.; Maser, W. K.; Bernier, P.; Loiseau, A.; Lamy de la Chapele, M.; Lefrant, S.; Deniard, P.; Lee, R.; Fisher, J. E. *Nature* **1997**, *383*, 756.

(4) Guo, T.; Nikolaev, P.; Thess, A.; Colbert, D. T.; Smalley, R. E. *Chem. Phys. Lett.* **1995**, *243*, 49.

(5) Ruoff, R. S.; Lorents, D. C.; Malhotra, R. *Nature* **1993**, *366*, 637.

(6) Maiti, A.; Brabec, C. J.; Roland, C.; Bernholc, J. *Phys. Rev., Condens. Mater.* **1997**, *55*, R6097.

(7) Kiang, C. H.; Goddard, W. A.; Beyers, R.; Salem, J. R.; Bethune, D. S. *Mater. Res. Soc. Symp. Proc.* **1995**, *359*, 69.

(8) Maiti, A.; Brabec, C. J.; Roland, C.; Bernholc, J. *Phys. Rev., Condens. Mater.* **1995**, *52*, 14850.

(9) Yudasaka, M.; Komatsu, T.; Ichihashi, T.; Achiba, Y.; Iijima, S. *J. Phys. Chem. B* **1998**, *102*, 4892.

(10) Yudasaka, M.; Ichihashi, T.; Iijima, S. *J. Phys. Chem. B* **1998**, *102*, 10201.

(11) Maser, W. K.; Munoz, E.; Beito, A. M.; Martinez, M. T.; Fuente, G. F.; Maniette, Y.; Anglarete, E.; Sauvajor, J. L. *Chem. Phys. Lett.* **1998**, *292*, 587.

(12) Rao, A. M.; Richter, E.; Bandow, S.; Chase, B.; Eklund, P. C.; Williams, K. A.: Fang, S.; Subbaswamy, K. R.; Menon, M.; Smalley, R. E.; Dresselhaus, G.; Dresselhaus, M. S. *Science* **1997**, *366*, 637.

(13) Iijima, S.; Yudasaka, M.; Yamada, R.; Bandow, S.; Suenaga, K.; Kokai, F.; Takahashi, K. *Chem. Phys. Lett.*, submitted for publication.

(14) Kinoshita, K. *Carbon, Electrochemical and Physicochemical Properties, 3*; John Wiley & Sons: New York, 1988; Chapter 2.2.

(15) Touloukian, Y. S.; DeWitt, D. P. *Thermophysical Properties of Matter, Thermal Radiative Properties, Nonmetallic Solids*; IFI/Plenum: New York, Washington, 1972; Vol 8.

(16) Steinback, J.; Braunstein, G.; Dresselhaus, M. S.; Venkatesan, T.; Jacobson, D. C. *J. Appl. Phys.* **1988**, *58*, 4374.

(17) Achiba, Y. Private communication.

(18) Brannon, J. H.; Lankard, A. L.; Baise, A. I.; Burns, F.; Kauffman, J. *J. Appl. Phys.* **1985**, *56*, 1984.

(19) Rohlfing, E. A. *J. Chem. Phys.* **1988**, *89*, 6103.

(20) A heat penetration depth (L) can be estimated from $L = 2[\kappa t]^{1/2}$ where "K" is diffusivity and "t" is time during which heat penetrates.[18] The estimated value of κ ($=\lambda/\rho C$) for graphite is 5.3×10^{-1} cm^2/s. The values of λ (thermal conductivity), ρ (density), and C (specific heat) of graphite are 2.62 J s^{-1} cm^{-1}, 2.25 g cm^{-3}, and 2.2 J g^{-1} K^{-1}, respectively.

(21) Baldwin, J. M. *J. Appl. Phys.* **1973**, *44*, 3362.

(22) Olstad, R. A.; Olander, D. R. *J. Appl. Phys.* **1975**, *46*, 1499.